The EMBO Journal vol.13 no.18 pp.4269–4277, 1994

Compartmentalization of SHC, GRB2 and mSOS, and hyperphosphorylation of Raf-1 by EGF but not insulin in liver parenchyma

Gianni M.Di Guglielmo[1], Patricia C.Baass, Wei-Jia Ou, Barry I.Posner[2] and John J.M.Bergeron[3]

Departments of Anatomy and Cell Biology, [1]Biochemistry and [2]Medicine, McGill University, Montreal, Quebec, Canada H3A 2B2

[3]Corresponding author

Communicated by J.Schlessinger

Rat liver parenchyma harbors equal numbers of epidermal growth factor (EGF) and insulin receptors. Following administration of a saturating dose of EGF (10 μg/100 g body weight), there was a rapid ($t_{\frac{1}{2}}$ ~1.1 min) internalization of receptor coincident with its tyrosine phosphorylation at residue 1173 and receptor recruitment of the adaptor protein SHC, its tyrosine phosphorylation and its association with GRB2 and the Ras guanine nucleotide exchange factor, mSOS, largely in endosomes. This led to a cytosolic pool of a complex of tyrosine-phosphorylated SHC, GRB2 and mSOS. It was demonstrated that these constituents were linked to Ras activation by the characteristic decrease in Raf-1 mobility on SDS–PAGE, which was maintained for 60 min after a single bolus of administered EGF. While insulin administration (15 μg/100 g body weight) led to insulin receptor β-subunit tyrosine phosphorylation and internalization, there was little detectable tyrosine phosphorylation of SHC, recruitment of GRB2, association of a complex with mSOS or any detectable change in the mobility of Raf-1. Therefore, in normal physiological target cells *in vivo*, distinct signaling pathways are realized after EGF or insulin receptor activation, with regulation of this specificity most probably occurring at the locus of the endosome.

Key words: endocytosis/signal transduction/tyrosine phosphorylation

Introduction

Liver parenchyma is a major target organ enriched in insulin and epidermal growth factor (EGF) receptors (R) (Kahn *et al.*, 1974; O'Keefe *et al.*, 1974; Bergeron *et al.*, 1980; Cohen *et al.*, 1982). Morphological, subcellular fractionation and biochemical studies with this system have been used as a physiologically relevant model to assess receptor trafficking (Geuze *et al.*, 1984), receptor activation (Kay *et al.*, 1986; Khan *et al.*, 1986) and the relationship between receptor compartmentalization, as a consequence of ligand-mediated receptor internalization, and signal transduction (Burgess *et al.*, 1992; Wada *et al.*, 1992). As a consequence of these studies, a major physiological substrate for the EGFR tyrosine kinase was uncovered and termed pyp55 (Wada *et al.*, 1992; or pp55 by Donaldson and Cohen, 1992), and has been proposed recently to be the SH2-containing adaptor protein SHC (Ruff-Jamison *et al.*, 1993). Overexpression of SHC has been shown to lead to cellular proliferation and transformation (Pelicci *et al.*, 1992), and coimmunoprecipitation studies have uncovered a link between SHC tyrosine phosphorylation and the activation of Ras (Rozakis-Adcock *et al.*, 1992). With respect to insulin action, the major substrate for the insulin receptor tyrosine kinase, IRS-1, has been identified and purified from liver parenchyma (Rothenberg *et al.*, 1991). Using Chinese hamster ovary (CHO) cells (Skolnik *et al.*, 1993b), COS-1 cells (Baltensperger *et al.*, 1993) or fibroblasts (Pronk *et al.*, 1993) transfected with the insulin receptor tyrosine kinase, insulin receptor activation and consequent tyrosine phosphorylation of IRS-1 have also been linked to the recruitment of GRB2 and the Ras guanine nucleotide exchange factor, mSOS, as well as the phosphorylation of SHC.

A convergence of signaling pathways from insulin and EGFR activation is remarkable since *in vivo* their physiological responses are different. In adult liver, the acute action of insulin is related to metabolic effects such as the regulation of glycogen formation and the consequent maintenance of blood glucose homeostasis (Mortimore *et al.*, 1967). Although less well defined, activation of the EGFR in adult liver has been linked to organ repair through increased mitogenesis (Marti *et al.*, 1989; Mead and Fausto, 1989; Jhappan *et al.*, 1990).

We have used a preparative subcellular fractionation approach to address receptor compartmentalization and signal transduction *in vivo*. We find major differences in the signaling pathways from the activated EGF and insulin receptors and demonstrate a complex of activated EGFR, phosphotyrosine-modified SHC, GRB2 and the Ras guanine nucleotide exchange factor mSOS in the endosomal membrane, as well as a complex of phosphotyrosine-modified SHC, GRB2 and mSOS in the cytosol. These events coincide with a reduced mobility of Raf-1 on SDS–PAGE, associated previously with Ras-dependent hyperphosphorylation and activation of Raf-1 (Morrison *et al.*, 1989; Wood *et al.*, 1992). These changes were not observed in rat liver subsequent to insulin administration.

Results

The injection of EGF or insulin into the portal circulation of young adult rats leads to the rapid autophosphorylation of their respective receptor kinases in liver parenchyma. Coincidentally, the receptors are internalized, without appreciable lag, into hepatic endosomes (Khan *et al.*, 1989; Lai *et al.*, 1989a,b; Burgess *et al.*, 1992; Wada

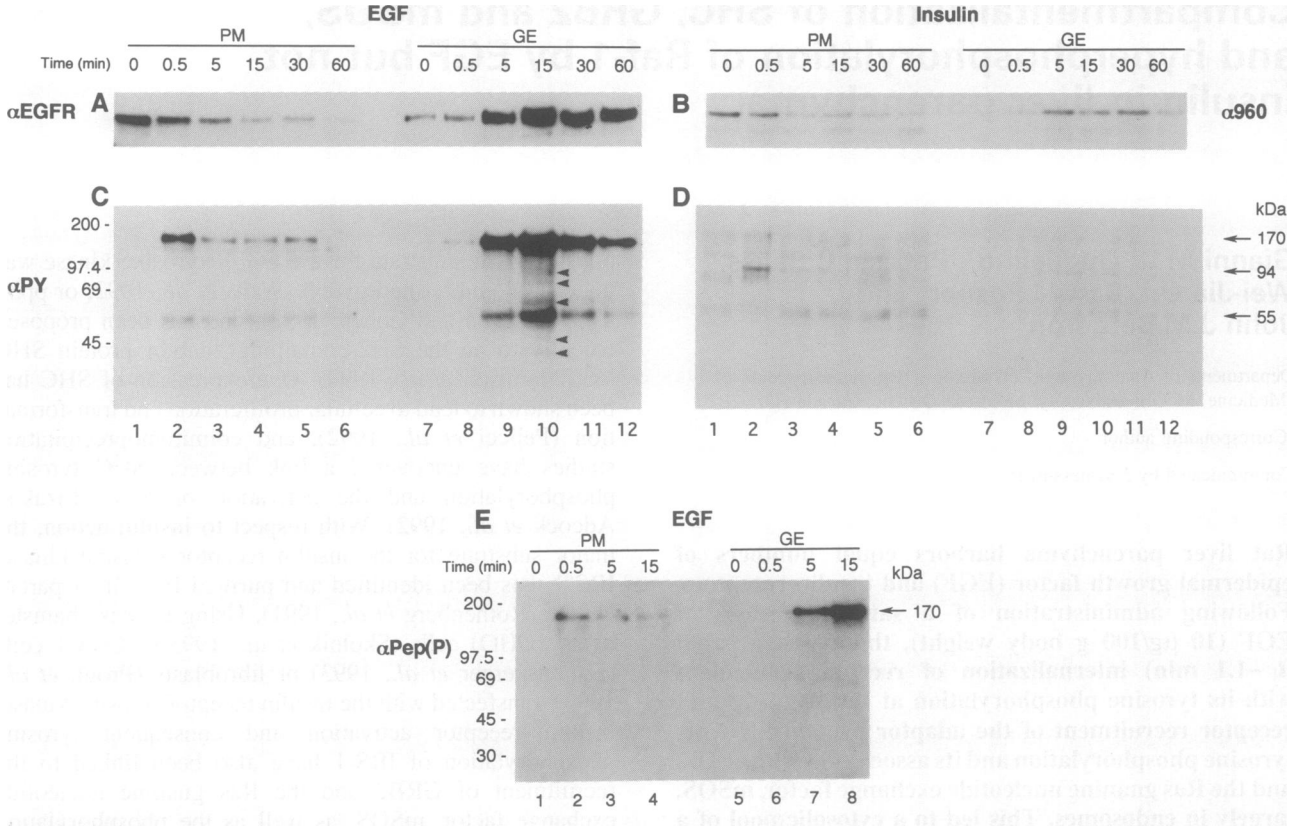

Fig. 1. Kinetics of EGF and insulin receptor signaling in plasma membranes and endosomes. Rat liver plasma membrane and GE fractions were isolated at the indicated times after EGF (10 μg/100 g body weight; **A**, **C** and **E**) or insulin (15 μg/100 g body weight; **B** and **D**) administration, and immunoblotted with polyclonal antibodies to a synthetic peptide comprising residues 1164–1176 of the EGFR (αEGFR; A; 18 h exposure) or the β-subunit of the insulin receptor (α960; B; 18 h exposure), or antibodies recognizing phosphotyrosine (αpy; C and D; 18 h exposure), or a phosphopeptide antibody which recognizes a phosphotyrosine peptide encompassing tyrosine 1173 of the EGFR [αPep(P); E; 48 h exposure]. Each lane contains 50 μg protein of plasma membrane or 25 μg protein of GE fraction. The mobilities of the EGFR (170 kDa), the β-subunit of the insulin receptor (94 kDa) and pyp55 (55 kDa) are indicated on the right. The arrowheads indicate phosphotyrosine-modified proteins of 95, 81, 66, 46 and 42 kDa found in the GE fraction in response to EGF. Molecular weights of the proteins were calculated from the relative mobilities of molecular mass markers (left).

et al., 1992). To evaluate the relationship between compartmentalization and signaling, we isolated hepatic subcellular fractions and evaluated them for the presence of tyrosine-phosphorylated and/or receptor-associated signaling molecules as a consequence of ligand administration.

Established protocols were followed to prepare plasma membrane and endosomal fractions (GE) which have been demonstrated to be free of cross contamination on the basis of electron microscopy, marker enzyme analysis and latency studies for ligand-mediated receptor activation (Kay *et al.*, 1986; Khan *et al.*, 1986, 1989; Lai *et al.*, 1989a,b; Wada *et al.*, 1992). Electron microscopy using a methodology to ensure random sampling demonstrated that all domains of the hepatic plasmalemma were present, including the sinusoidal surface and coated pits (not shown). No endosomes were evident in plasma membrane fractions, although uncoated vesicular profiles of 70 nm diameter were closely associated with the cytosolic surface of plasmalemmal sheets. In contrast, the endosomal fraction was enriched in lipoprotein-filled endosomes as well as Golgi saccules, and was therefore designated as the GE fraction (not shown).

After administration of a single receptor-saturating dose of EGF (10 μg/100 g body weight) or insulin (15 μg/100 g body weight), receptor internalization was rapid and extensive (Figure 1A and B) as described previously (Burgess *et al.*, 1992; Wada *et al.*, 1992). Despite the similarities in the rapidity and extent of receptor internalization, differences were observed in the tyrosine-phosphorylated proteins induced by the respective ligands (see Figure 1C and D).

The administration of EGF led to the strong tyrosine phosphorylation of two polypeptides, of 170 and 55 kDa (Figure 1C), demonstrated previously to be the phosphorylated EGFR and its major associated substrate pyp55 (Donaldson and Cohen, 1992; Wada *et al.*, 1992). Both the EGFR and pyp55 were phosphorylated maximally at 30 s in the plasma membrane, while peak phosphotyrosine content of these two proteins was observed at 15 min in endosomes (Figure 1C, lane 10). Other less prominent phosphotyrosine-modified proteins were evident in the GE fraction in response to the receptor-saturating dose of EGF (10 μg/100 g body weight), as indicated by arrowheads. In contrast, insulin administration led to a rapid (within 30 s) and brief burst of tyrosine autophosphorylation of the 94 kDa β-subunit of the insulin receptor (Figure 1D, lane 2). The protein was also tyrosine-phosphorylated, but to a lower level, in isolated endosomes (GE) (Figure 1D, lanes 8–12) as described by Burgess *et al.* (1992).

The major site of EGFR activation *in vivo* is phosphotyrosine 1173 (Downward *et al.*, 1984). It was verified

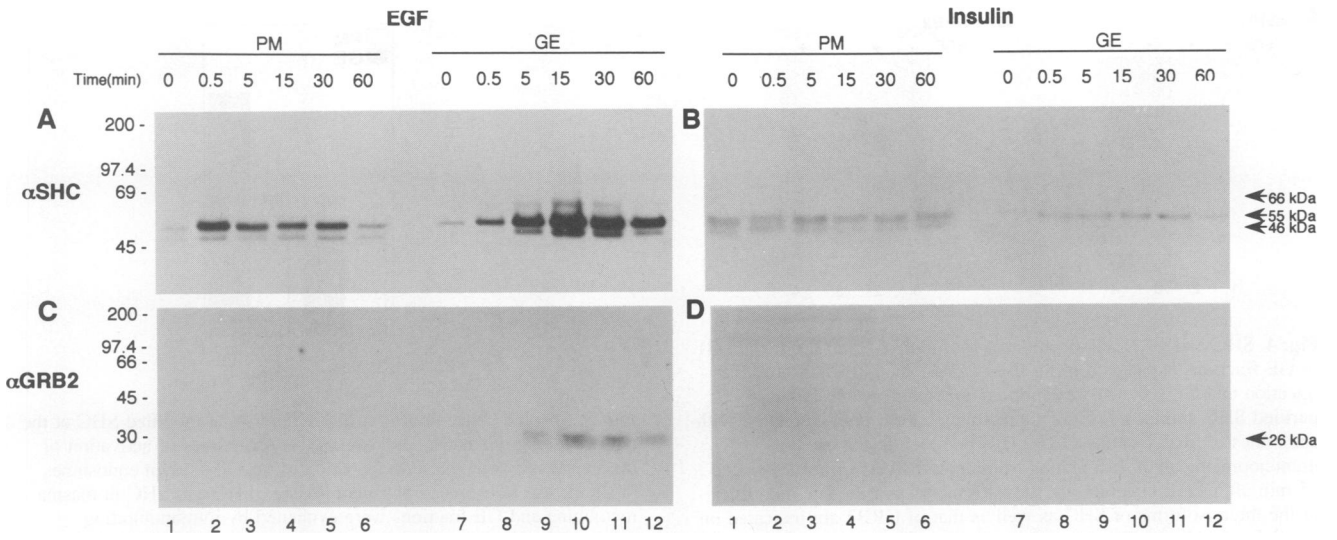

Fig. 2. Kinetics of SHC and GRB2 recruitment to plasma membranes and endosomes after EGF or insulin administration. Rat liver plasma membrane and GE fractions isolated at the indicated times after EGF or insulin administration were immunoblotted with antibodies to SHC (**A** and **B**) or GRB2 (**C** and **D**). 50 μg plasma membrane protein and 25 μg GE protein were applied to each lane. The molecular masses of the three isoforms of SHC (A) and the mobility of GRB2 (B) are indicated on the right. Exposures were 6 h for (A) and (B) and 48 h for (C) and (D).

that liver parenchyma EGFR was tyrosine-phosphorylated at this site, in response to EGF stimulation, by immunoblotting plasma membrane and GE fractions with the phosphopeptide-specific antibody [Pep(P)] described by Bangalore *et al.* (1992) (Figure 1E). The phosphorylation of tyrosine 1173 of the EGFR defines the major motif for the recruitment of the adaptor protein SHC (Batzer *et al.*, 1994). Hence, SHC recruitment to plasma membranes and endosomes was evaluated as a function of EGF and insulin administration *in vivo* (Figure 2A and B). Two polypeptides, of 46 and 55 kDa, were found to associate with the plasma membrane fraction in an EGF-dependent manner (Figure 2A, lanes 1–6). These correspond in mobility to two isoforms of SHC described previously by Pelicci *et al.* (1992). In the GE fraction a stronger and more prolonged signal for these two polypeptides was observed, as well as the presence of the 66 kDa form of SHC (Figure 2A). The 55 and 66 kDa forms of SHC corresponded exactly in mobility to major tyrosine-phosphorylated polypeptides found in the GE fraction at 15 min (see Figure 1C, lane 10, and Figure 2A, lane 10). In contrast, the recruitment of SHC to plasma membranes and endosomes following insulin administration was markedly lower (Figure 2B).

The SH2–SH3-containing adaptor protein GRB2 has been demonstrated to associate with phosphotyrosine-modified SHC (Rozakis-Adcock *et al.*, 1992). In addition, GRB2 has been shown to associate with the motif at phosphotyrosine 1068 of the EGFR and less so with that at phosphotyrosine 1086 (Batzer *et al.*, 1994). We therefore evaluated GRB2 recruitment to the plasma membrane and GE fractions in response to EGF and insulin *in vivo*. After EGF administration, recruitment was mainly found to the GE fraction, with little association observed in the plasma membrane fraction (Figure 2C). After insulin administration no detectable GRB2 was found associated with either plasma membrane or GE fractions (Figure 2D).

Although these data demonstrate endosomes as a site of EGFR accumulation and concentration of the adaptors SHC and GRB2, they do not demonstrate physical associ-

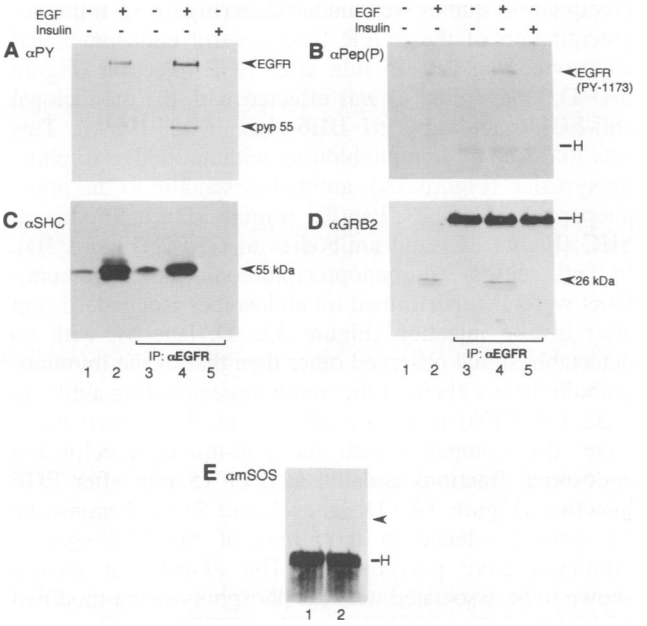

Fig. 3. Activated EGFR is associated with phosphotyrosine–SHC and GRB2/mSOS in endosomes. GE fractions isolated from control rat liver homogenates (lanes 1) or from liver homogenates prepared 15 min after EGF administration (lanes 2) were immunoblotted with antibodies to phosphotyrosine (**A**), Pep(P) (**B**), SHC (**C**) or GRB2 (**D**). The bands are compared with those revealed after immunoprecipitation (EGFR monoclonal antibody IgG 151 BH-6) of GE fractions isolated from control liver homogenates (lane 3, A–D), GE fractions prepared from liver homogenates 15 min after the injection of EGF (lane 4, A–D) or 15 min after the injection of insulin (lane 5, A–D). The mobilities of the EGFR, the 55 kDa isoform of SHC and GRB2 (26 kDa) are indicated by the arrowheads on the right of each panel. αEGFR immunoprecipitates from GE fractions isolated from control liver homogenates (lane 1) or GE fractions isolated 15 min after EGF injection (lane 2) were immunoblotted with mSOS antibodies (**E**). The mobility of mSOS is indicated by the arrowhead. The cross-reactivity between immunoblotting IgG and immunoprecipitating IgG heavy chain is indicated (H). (A), (D) and (E) are from immunoblots using alkaline phosphatase-conjugated secondary antibodies visualized by blot immunostaining as described in Materials and methods. (B) and (C) are of immunoblots visualized with [^{125}I]goat anti-rabbit antiserum (B, exposure 48 h; C, exposure 6 h).

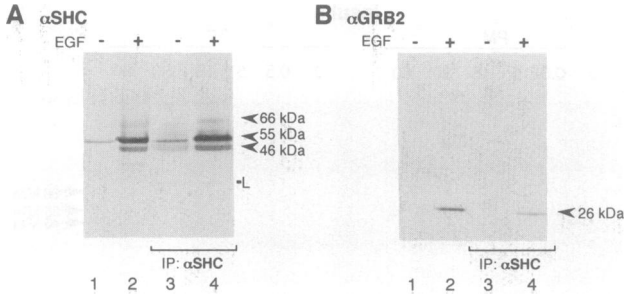

Fig. 4. SHC and GRB2 association in endosomes. Control GE (lane 3) or GE fractions isolated from rat liver homogenates 15 min after the injection of EGF (lane 4) were immunoprecipitated with affinity-purified SHC antibodies. Immunoprecipitates were immunoblotted with antibodies to SHC (**A**) and GRB2 (**B**). For each panel the non-immunoprecipitated GE fractions from control livers or those isolated 15 min after EGF injection are shown (lanes 1 and 2). The mobilities of the three isoforms of SHC as well as that of GRB2 are indicated on the right of (A) and (B), respectively. Immunoblots were visualized by immunostaining with alkaline phosphatase-conjugated secondary antibody. The cross-reactivity between immunoblotting IgG and immunoprecipitating IgG light chain is indicated (L).

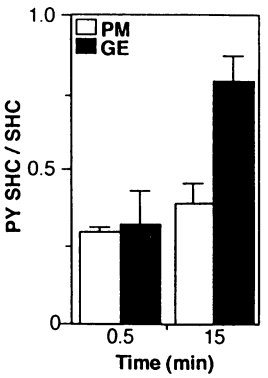

Fig. 5. Specific concentration of phosphotyrosine-modified SHC at the plasma membrane and in endosomes. At peak times of activation of the EGFR tyrosine kinase at the cell surface (30 s) or in endosomes (15 min), the contents of phosphotyrosine−SHC and SHC in plasma membrane and GE fractions were evaluated by immunoblotting followed by phosphoimager analysis (15 min exposure for immunoblots probed with anti-SHC and 80 min for anti-phosphotyrosine). The results represent the mean ±·SD (n = 3 fractionations).

ation among these molecules. Accordingly, coimmunoprecipitation studies were undertaken (Figure 3). Immunoprecipitation of the EGFR from control endosomes and endosomes isolated 15 min after EGF injection (Figure 3A−D, lanes 3 and 4) was effected with the monoclonal anti-EGFR antibody 151 BH6 (Lai *et al.*, 1989a). This was followed by immunoblotting with antibodies to phosphotyrosine (Figure 3A), antibodies specific to the phosphopeptide [PY-1173, Pep(P)] (Figure 3B), antibodies to SHC (Figure 3C) and antibodies to GRB2 (Figure 3D). In all cases, immunoprecipitations and immunoblots were also performed on endosomes isolated 15 min after insulin injection (Figure 3A−D, lane 5), with no detectable signal observed other than that of the immunoglobulin heavy chain of the immunoprecipitating antibody (IgG 151 BH6) in Figure 3B and D. The observations were also compared with the non-immunoprecipitated endosomal fractions isolated at 0 or 15 min after EGF injection (Figure 3A−D, lanes 1 and 2) to demonstrate the correspondence in mobilities of the EGF-specific immunoreactive polypeptides. The EGFR was clearly shown to be associated with the phosphotyrosine-modified 55 kDa isoform of SHC, as well as GRB2 in endosomes, in a ligand-specific manner. Since a complex of activated EGFR with the Ras guanine nucleotide exchange factor mSOS has been demonstrated to be involved in Ras activation, we also probed for mSOS in the complex. As shown in Figure 3E, an EGF-dependent association of mSOS was found in immunoprecipitates of the EGFR.

To evaluate if these constituents were part of the same complex or if complexes of SHC and the EGFR were distinct from those of the EGFR in association with pyp55 or GRB2, immunoprecipitation of solubilized endosomes with antibody to SHC was followed by immunoblotting with antibodies to SHC (Figure 4A), GRB2 (Figure 4B) or phosphotyrosine (not shown). All isoforms of SHC, as well as the adaptor protein GRB2, were found in the immunoprecipitate in an EGF-dependent manner. Hence, phosphotyrosine-modified SHC, GRB2, mSOS and the activated EGFR were in oligomeric association in the same complex in the endosomal membrane.

Since pyp55 is the major *in vivo* substrate of the EGFR (Donaldson and Cohen, 1992; Wada *et al.*, 1992) and corresponds to phosphotyrosine-modified SHC (see Ruff-Jamison *et al.*, 1993), we compared by phosphoimager analysis the extent of phosphotyrosine modification of SHC at peak times of EGFR activation in the plasma membrane (30 s) or in endosomes (15 min). Quantitation (Figure 5) revealed a significantly higher ($P < 0.001$) phosphotyrosine content of SHC in endosomes. This is consistent with recruitment of SHC at the plasma membrane and tyrosine phosphorylation of a proportion of recruited SHC by the cell surface EGFR. The higher proportion of phosphorylated SHC in endosomes is due to continuing tyrosine phosphorylation occurring upon internalization and/or the loss by dissociation of unphosphorylated SHC.

The quantitative contribution of the plasma membrane and endosomal compartments to signal transduction via the EGFR may be considered by accounting for the yields and recoveries of the respective subcellular fractions. Quantitation was therefore carried out as described in Materials and methods. Ligand-dependent translocation of the EGFR from plasma membranes to endosomal membranes was rapid, with an initial $t_{\frac{1}{2}}$ of 1.1 ± 0.3 min and with 66% of the receptor internalized by 5 min (Figure 6A). The phosphotyrosine content of the plasma membrane EGFR peaked transiently at 30 s, but was maintained at significant levels over that of zero time, up to 30 min after EGF administration (Figure 6B).

The majority of phosphotyrosine-modified EGFR was, however, found in endosomes with increased phosphorylation over that found at the plasma membrane at 30 s, as reported previously by Wada *et al.* (1992) using a different approach (direct ^{32}P-labeling *in vivo*).

The level of the 55 kDa isoform of SHC in these particulate compartments was not as predicted from that of tyrosine-phosphorylated EGFR (Figure 6C). Most recruitment was found at the plasma membrane within 30 s of EGF administration. From 15 to 60 min after EGF administration, the SHC content of endosomes and plasma membrane was identical. However, the relative content of

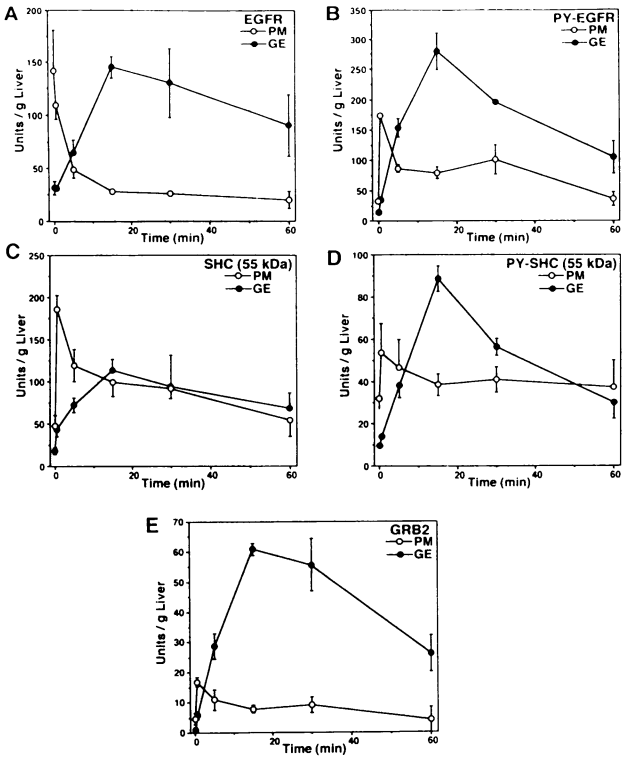

Fig. 6. Kinetics of EGFR internalization, activation, recruitment of SHC, tyrosine phosphorylation of SHC and recruitment of GRB2. Quantitation by phosphoimager analysis of the content of the EGFR (**A**; exposure 60 min), the phosphotyrosine-modified EGFR (**B**; exposure 80 min), the 55 kDa isoform of SHC (**C**; exposure 15 min), the phosphotyrosine-modified 55 kDa isoform of SHC (**D**; exposure 80 min) and the adaptor protein GRB2 (**E**; exposure 2 h) in plasma membrane and GE fractions at the indicated times after EGF administration. Each point is the mean of three separate experiments ± SD and is expressed as arbitrary phosphoimager units ($\times 10^{-3}$) per gram liver, corrected for yields and recoveries as described in Materials and methods.

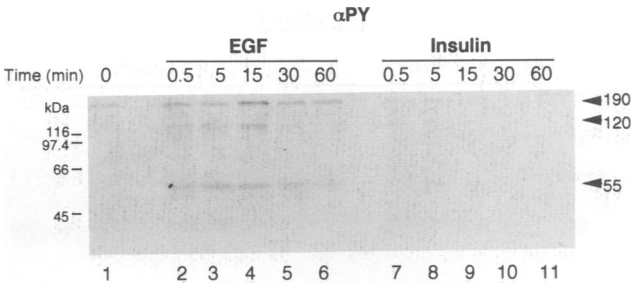

Fig. 7. Kinetics of appearance of cytosolic tyrosine-phosphorylated proteins after EGF or insulin administration. 300 μg of control rat liver cytosol (0 min) or cytosol isolated from liver homogenates at 0.5–60.0 min after the administration of EGF (lanes 2–6) or insulin (lanes 7–11), were resolved by SDS−PAGE and immunoblotted with antiphosphotyrosine antibodies (exposure 6 h). The cytosolic protein molecular masses of pyp55, pyp120 and pyp190 were calculated from the mobilities of molecular mass markers (left) and are indicated on the right.

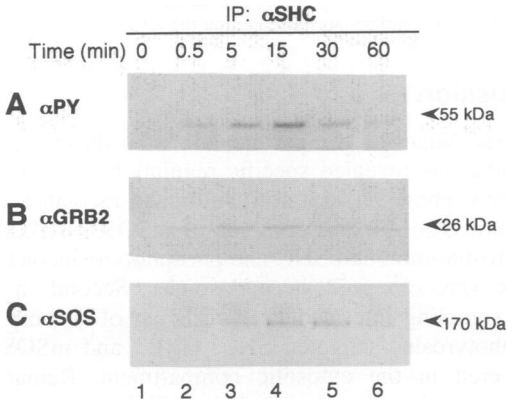

Fig. 8. EGF-dependent association of phosphotyrosine−SHC with GRB2/mSOS in the cytosol. Cytosolic fractions were isolated after the EGF administration and immunoprecipitated with affinity-purified antibodies raised to SHC. The immunoprecipitates were immunoblotted with antibodies specific for phosphotyrosine (**A**), GRB2 (**B**) or mSOS (**C**), with their respective molecular masses indicated on the right.

tyrosine-phosphorylated SHC (Figure 6D) did reflect that of the phosphorylated EGFR (see Figures 1C and 6D), thereby accounting for the higher level of tyrosine phosphorylation of SHC in endosomes at 15 min as compared with plasma membrane at 30 s (Figure 5).

Quantitation demonstrated that GRB2 association was largely with endosomes, as opposed to plasma membranes, with a 3- to 5-fold higher level of GRB2 association in endosomes at 15 min as opposed to that in plasma membrane at 30 s. Nevertheless, a significant signal was detected in plasma membrane which was maintained above that at zero time for at least 30 min (Figure 6E).

Although the EGFR is exclusively membrane-bound, several of its associated substrates, i.e. GRB2 and SHC, are largely cytosolic. We therefore evaluated the cytosolic compartment for the content of tyrosine-phosphorylated proteins after EGF administration (Figure 7, lanes 2–6). Of the three major proteins which were tyrosine-phosphorylated, two were EGF-specific (120 and 55 kDa) and one was constitutively present (190 kDa) and also found unchanged after insulin injection (Figure 7, lanes 7–11). Following immunoprecipitation with anti-SHC antibody of liver cytosol isolated at 0–60 min after EGF administration, the 55 kDa phosphopeptide was shown to correspond to the tyrosine-phosphorylated 55 kDa isoform of SHC, as evaluated by immunoblotting with antiphosphotyrosine (Figure 8A) and anti-SHC antibodies (not shown). GRB2 was coprecipitated with the same kinetics of association as found for the tyrosine-phosphorylated SHC in cytosol (Figure 8B), and mSOS was also found to coimmunoprecipitate (Figure 8C).

The signaling molecules identified in liver parenchyma following EGF administration have been shown in a variety of other systems to result in Ras activation (reviewed by McCormick, 1993). Evaluation of the GTP content of Ras *in vivo* presents experimental difficulties with respect to the specific radioactivities of [^{32}P]GTP pools following ^{32}P administration. We elected to assess Ras activation by following the mobility shift of Raf-1 in SDS−PAGE, which has been proposed to reflect Ras-dependent Raf-1 activation (Morrison *et al.*, 1989; Wood *et al.*, 1992; Ueki *et al.*, 1994). After EGF or insulin administration, Raf-1 was found to be predominantly cytosolic. The assessment of cytosolic Raf-1 (Figure 9) clearly revealed a mobility shift in Raf-1 from 5 to 60 min after the administration of a single bolus of EGF (Figure 9, lanes 3–6), but not after insulin administration (Figure 9, lanes 7–12).

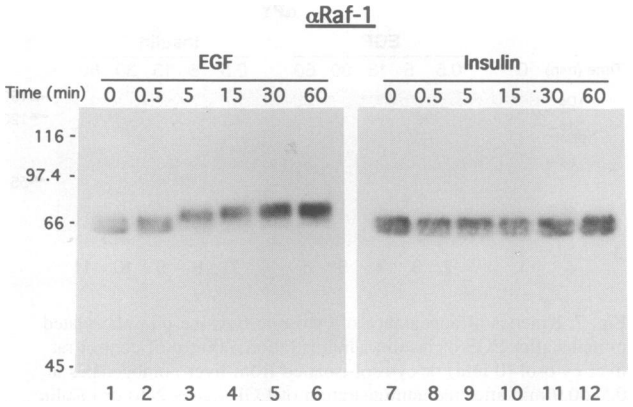

Fig. 9. Mobility of Raf-1 in SDS−PAGE after EGF or insulin administration. Rat liver cytosolic fractions were isolated at the indicated times after EGF (lanes 1–6) or insulin (lanes 7–12) administration and immunoblotted with αRaf-1 antibodies. A change in mobility of Raf-1 is evident from 5 to 60 min after EGF administration, but is undetectable after insulin administration. Molecular mass markers are indicated on the left.

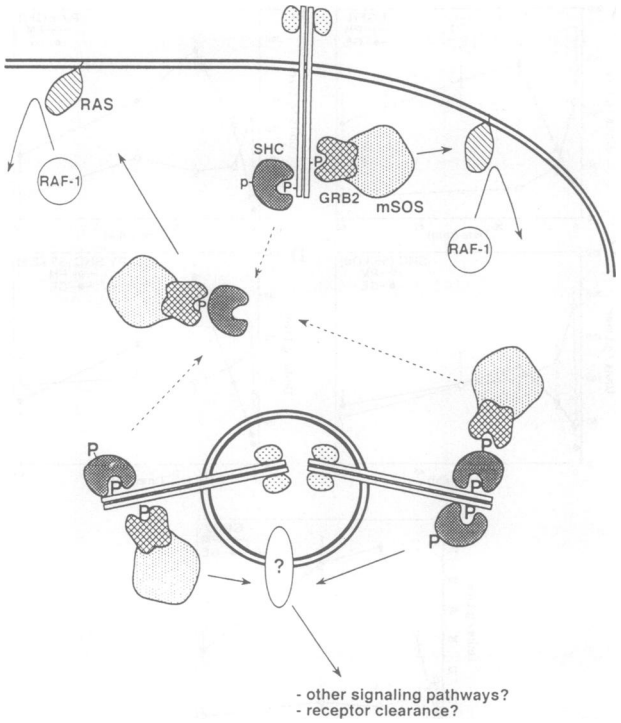

Fig. 10. Compartmentalization of the EGFR signal transduction pathway *in vivo*. EGFR activation leads to the recruitment of SHC and its tyrosine phosphorylation. Ligand-mediated receptor internalization results in maximal tyrosine phosphorylation of SHC and association with GRB2/mSOS on the endosomal membrane. This in turn leads to the generation of a cytosolic pool of phosphorylated SHC−GRB2/mSOS. The activation of Ras and the hyperphosphorylation of Raf-1 are considered a consequence of both a direct physical association with the activated EGFR mediated by adaptors, as well as a cytosolic pool of tyrosine-phosphorylated SHC−GRB2/mSOS. Dashed arrows refer to the postulated dissociation of signaling molecules from the activated EGFR to the cytosol. Solid arrows refer to direct protein−protein interactions.

Discussion

The assessment of compartmentalization during receptor signaling has revealed specific regulation *in vivo* during the early phases (0–15 min) of ligand-mediated EGFR internalization. First, a complex of mSOS, GRB2, phosphotyrosine-modified SHC and phosphotyrosine-activated EGFR was observed in endosomes. Second, a long-lived signaling intermediate, consisting of a complex of phosphotyrosine-activated SHC, GRB2 and mSOS, was uncovered in the cytosolic compartment. Remarkably, though tyrosine phosphorylation of SHC and association with GRB2/mSOS was demonstrated to be a consequence of the activated EGFR, no comparable activation of these constituents was seen by the insulin receptor in liver parenchyma *in vivo*. Third, the specificity of signaling was clearly demonstrated by the prolonged hyperphosphorylation of Raf-1, as evaluated by its characteristic mobility shift in SDS−PAGE after EGF but not insulin administration. A single bolus of a saturating dose (10 μg/100 g body weight) of EGF administered intraportally is rapidly cleared from the circulation with a $t_{\frac{1}{2}}$ of <5 min (Figure 8 of Lai *et al.*, 1989a). We suggest that this relatively rapid ligand clearance translates into extended signal transduction consequent to ligand-mediated EGFR translocation to endosomes and the generation of a cytosolic pool of a complex of activated SHC−GRB2 and −mSOS. This cytosolic complex was maintained for 5–60 min after a single dose of EGF (Figure 8). This finding was unexpected since Ruff-Jamison *et al.* (1993) have concluded that SHC in liver cytosol was exclusively monomeric and largely non-tyrosine-phosphorylated after EGF administration. The observed differences are probably due to the greater concentration of cytosolic protein analyzed in our study, as compared with those of Ruff-Jamison *et al.* (1993), as well as our use of coimmunoprecipitation to evaluate GRB2−mSOS associations directly.

Electron microscopy, marker enzyme analysis (Bergeron *et al.*, 1986; Khan *et al.*, 1986), the direct visualization of internalized [^{125}I]EGF by quantitative electron microscopy radioautography (Figures 2 and 3 of Lai *et al.*, 1989b), latency studies for receptor kinase stimulation (Kay *et al.*, 1986) and proteinase sensitivity assays (Wada *et al.*, 1992) have all established that the endosome preparation is minimally contaminated by plasma membrane fragments. Endosomes were the major particulate compartment which recruited GRB2 in response to EGF (Figure 6E). The complex of PY-1173-activated EGFR; phosphotyrosine-modified SHC, GRB2 and mSOS represent the first evidence for such a complex *in vivo*. The physiological relevance of this complex is probably related to Ras activation. GRB2 has been demonstrated to activate Ras via a direct physical linkage with activated receptor and the Ras guanine nucleotide exchange factor mSOS (Lowenstein *et al.*, 1992; Buday and Downward, 1993; Chardin *et al.*, 1993; Egan *et al.*, 1993; Gale *et al.*, 1993; Li *et al.*, 1993; Olivier *et al.*, 1993; Rozakis-Adcock *et al.*, 1993; Simon *et al.*, 1993). Although endosomes are a major site of GRB2 recruitment and SHC phosphorylation, lower but significant levels of both proteins were found associated with plasma membranes up to 30 min post-injection of EGF. As shown in Figure 10, we propose that the prolonged hyperphosphorylation of Raf-1 (from 5 to 60 min; Figure 9) in response to EGF may be due to the pool of cytosolic signaling constituents most probably

emanating from endosomes at times >5 min. Such a scenario provides a rationale for the adaptor protein SHC, since this constituent is not a membrane protein and is able to form a signaling complex in the cytosol following its tyrosine phosphorylation.

The comparatively low level of GRB2 recruited to the activated plasma membrane EGFR may be related to receptor trafficking. For high efficiency internalization via coated pits, two regions in the cytosolic tail of the EGFR, corresponding to residues 993–1022 and 1024–1186, have been shown independently to restore ligand-mediated high efficiency internalization to receptors truncated at residue 958 (Chang *et al.*, 1993). The latter region, comprising residues 1024–1186, contains the major sites of tyrosine autophosphorylation (Downward *et al.*, 1984; Hsuan *et al.*, 1989; Margolis *et al.*, 1989; Walton *et al.*, 1990) and recruitment of SHC and GRB2. Since the activated EGFR also associates at the cell surface with the clathrin-coated pit adaptin AP-2 (Sorkin and Carpenter, 1993), this may lead to competition with the recruitment and/or tyrosine phosphorylation of SH2-signaling adaptors to the EGFR. We suggest that this may be responsible for the low level of GRB2 recruitment to the activated EGFR at the cell surface. The positioning of AP-2 on the EGFR may also diminish access of SHC to the EGFR kinase domain, while still allowing SHC recruitment to PY-1173 of the EGFR. This could account for the high level of SHC recruitment but lower level of SHC tyrosine phosphorylation seen at the cell surface.

Tyrosine kinase activity of the EGFR has also been demonstrated to regulate whether internalized EGFR in the endosomal membrane is targeted back to the plasma membrane for recycling or into the intravesicular content of multivesicular endosomes for down-regulation. Felder *et al.* (1990) showed that a kinase-defective point mutant of the EGFR was able to access the boundary of the endosomal membrane following receptor internalization, but was prevented from gaining access to the intraluminal microvesicle population of multivesicular endosomes. They postulated that EGFR tyrosine phosphorylation of endosomal substrates may regulate this sorting event. The complex of activated EGFR, tyrosine-phosphorylated SHC and GRB2 represents a relevant candidate for the above, as well as having a role, albeit poorly defined, in signal transduction at this locus (Figure 10).

Burgess *et al.* (1992) have demonstrated that insulin-mediated receptor internalization leads to a diminution of its phosphotyrosine content as confirmed here. However, the endosomal insulin receptor remains activated, i.e. with an increased V_{max} in its tyrosine kinase activity (Khan *et al.*, 1989). Hence, analogous to pp60–c-src activation, a model of dephosphorylation of the insulin receptor coupled with its activation has been proposed (Burgess *et al.*, 1992). Dephosphorylation and activation coincided with internalization (Burgess *et al.*, 1992). It is therefore relevant that Kelly and Ruderman (1993) have shown, in fat cells, the major *in vivo* substrate of the insulin receptor kinase, IRS-1, was tyrosine-phosphorylated in response to insulin and compartmentalized to low density membranes which could be distinguished from plasma membranes.

In studies employing insulin receptors transfected into CHO cells, COS-1 cells or fibroblasts, tyrosine phosphorylation of SHC and activation of GRB2 have been demonstrated (Baltensperger *et al.*, 1993; Pronk *et al.*, 1993; Skolnik *et al.*, 1993a,b). Raf-1 activation has also been demonstrated in CHO cells overexpressing human insulin receptors (e.g. Ueki *et al.*, 1994). Despite the similar number of insulin and EGF receptors in liver parenchyma of young adult male rats (Burgess *et al.*, 1992; Wada *et al.*, 1992), SHC phosphorylation and association with GRB2 and mSOS was not observed in response to insulin, nor was any mobility shift in Raf-1 observed. We postulate that liver parenchyma has evolved endosomally located mechanisms to regulate the specificity of insulin and EGFR signal transduction. One of these regulatory mechanisms may be at the level of intra-endosomal ligand degradation. Whereas liver endosomes contain a potent acidic insulinase activity (Doherty *et al.*, 1990; Authier *et al.*, 1994), little EGF degradation has been observed therein (Doherty *et al.*, 1990). Indeed, most EGF is receptor-bound in endosomes (Lai *et al.*, 1989b). Degradation of insulin in endosomes would limit the temporal window of insulin receptor activation in this compartment especially since endosomes contain phosphotyrosine phosphatase(s) with potent activity directed against the tyrosine-phosphorylated insulin receptor (Faure *et al.*, 1992). Backer *et al.* (1990) have observed that the endosomal insulinase is absent from CHO cells. We suggest that this accounts, at least in part, for the enhanced tyrosine phosphorylation of SHC and GRB2/SOS activation of Ras observed in insulin receptor-transfected CHO cells. Regulation of signal transduction at the level of the endosome may discriminate between the metabolic versus the mitogenic consequences of insulin receptor activation.

Materials and methods

Receptor-grade EGF was purchased from Collaborative Research Inc. (Lexington, MA) and insulin was obtained from Eli Lilly (Indianapolis, IN). All other reagents were purchased from Sigma (St Louis, MO), Anachemia (Montreal, Quebec, Canada) and Fisher Scientific (Montreal, Quebec, Canada). Male Sprague–Dawley rats (100–120 g body weight) were purchased from Charles River (St Constant, Quebec, Canada).

Antibodies

Polyclonal antibodies raised to the SH2 domain (residues 366–473) of SHC, as well as the *Escherichia coli*-expressed pGEX–SHC SH2 vector, were obtained from Drs J.McGlade and T.Pawson (Samuel Lunenfeld Research Institute, University of Toronto, Canada). The *E.coli*-expressed protein was purified by glutathione–agarose beads (Pharmacia, Baie d'Urfe) and antisera were raised to the glutathione-eluted protein by injection into rabbits as described by Pelicci *et al.* (1992). The anti-SHC antibody was affinity-purified using the bacterially expressed fusion protein coupled to CB–Sepharose beads (Pharmacia, Baie d'Urfe). Monoclonal antibodies raised to phosphotyrosine and GRB2 were purchased from Sigma and Transduction Laboratories (Lexington, KY), respectively. Affinity-purified polyclonal antibodies to Raf-1 were purchased from Santa Cruz Biotechnology Inc. (Santa Cruz, CA) and the mSOS polyclonal antibodies were purchased from UBI (Lake Placid, NY). Antibodies raised to a tyrosine phosphopeptide (residues 1247–1260) of the activated neu receptor, Pep(P), as described by Bangalore *et al.* (1992), were obtained from Dr D.Stern (Department of Pathology, Yale University). The monoclonal IgG 151 BH-6 EGFR antibody used in immunoprecipitations and polyclonal antibodies to a synthetic peptide (residues 1164–1176) of the EGFR used for immunoblotting were as described in Wada *et al.* (1992). Polyclonal antibodies raised to a synthetic peptide (residues 942–969) of the β-subunit of the insulin receptor were used as described by Burgess *et al.* (1992). [^{125}I]Goat anti-rabbit and [^{125}I]goat anti-mouse secondary antibodies were purchased from DuPont NEN (Mississauga, Ontario, Canada) and ICN Biomedicals Inc. (Irvine, CA), respectively. The goat anti-mouse (Fc-specific) secondary antibody conjugated to alkaline phosphatase

was purchased from Sigma. The goat anti-mouse and goat anti-rabbit secondary antibodies, conjugated to alkaline phosphatase, were purchased from Cappel Research Products (Durham, NC).

Subcellular fractionation

The isolation of plasma membrane and endosomal (GE) fractions was carried out as described by Kay *et al.* (1986) and Wada *et al.* (1992) with minor modifications. Male Sprague–Dawley rats (100–120 g body weight) were fasted for 14–16 h and injected into the hepatic portal vein with 10 μg EGF/100 g body weight or 15 μg insulin/100 g body weight. Animals were sacrificed and livers were rapidly removed and minced in ice-cold homogenization buffer (0.25 M sucrose, 20 mM Tris–HCl, pH 7.4, 1 mM $MgCl_2$, 4 mM NaF, 100 μM Na_3VO_4, 2 mM benzamidine, 5 mM iodoacetemide, 5 mM *p*-nitrophenyl phosphate, 165 kIU/ml aprotinin, 0.5 mM phenylmethylsulfonyl fluoride). All subsequent steps, including centrifugations, were carried out at 4°C and all buffers contained the protease and phosphatase inhibitors as stated above.

To isolate the total particulate (TP) and cytosolic (Cyt) fractions, livers were homogenized using a Potter–Elvehjem homogenizer to a final concentration of 5 ml/g liver. The TP and Cyt fractions were generated by centrifuging the homogenate at 100 000 *g* for 1 h and resuspending the pellet (TP) in homogenization buffer. The resultant supernatant (Cyt) was collected and frozen (−80°C).

To isolate the plasma membrane fractions, livers were homogenized using a Dounce homogenizer (B pestle) to a final concentration of 5 ml/g liver. Homogenates were centrifuged at 280 *g* for 5 min (Sorvall SS-34 rotor) to obtain a pellet (P1) and a supernatant (S1). The pellet was resuspended in half the original volume using the Dounce homogenizer and centrifuged at 280 *g* for 5 min to obtain P2 and S2. S2 was combined with S1 and centrifuged at 1500 *g* for 10 min to obtain P3 and S3. Pellets P2 and P3 were combined and resuspended and the molarity was adjusted to 1.42 M sucrose. This homogenate was overlaid with 0.25 M sucrose and centrifuged at 82 000 *g* for 1 h (Beckman SW 28 rotor). The pellicule at the 0.25–1.42 M interface was collected, the molarity adjusted to 0.39 M and centrifuged at 1500 *g* for 10 min (Sorvall SS-34). The plasma membrane was resuspended in homogenization buffer. A yield of 3.5 ± 0.8 mg protein/g liver weight was recovered over 17 experiments. The yield was identical to that described by Kay *et al.* (1986).

Endosomal (GE) fractions were isolated by centrifuging 20% liver homogenates for 10 min at 1500 *g* (Sorvall SS-34 rotor). The supernatant was centrifuged at 200 000 *g* for 30 min (Beckman 60 Ti rotor) and the microsomal pellet was resuspended to 1.15 M sucrose. This resuspension was overlaid with 1.00 and 0.25 M sucrose cushions and centrifuged at 200 000 *g* for 1.5 h (Beckman SW28 rotor). The GE fraction was collected at the 0.25–1.00 M sucrose interface and stored at −80°C. The yield of GE fraction was 0.40 ± 0.09 mg protein/g liver (n = 18) and similar to that described by Wada *et al.* (1992).

Yields and recoveries of subcellular fractions

The yield of the TP fraction was 68.2 ± 8.8 mg cell fraction protein/g liver (n = 17). The EGFR content was determined by quantitative immunoblotting. This was evaluated over the linear range of quantitative immunoblotting (between 25 and 125 μg TP protein) by phosphoimager analysis (2.54 ± 0.26 U/mg cell fraction protein for a 60 min exposure) and was unchanged from 0 to 60 min after EGF injection.

The mean EGFR content of plasma membrane fractions isolated at 0 time and 15 min after EGF injection was determined as 12.2 ± 3.4 and 2.40 ± 0.02 U/mg protein, respectively, by phosphoimager analysis. For the GE fraction isolated at 0 and 15 min post-EGF injection, the values were 12.8 ± 2.5 and 57.8 ± 4.1 U/mg cell fraction protein, respectively. From the respective yields of the plasma membrane and GE fractions (i.e. 3.5 ± 0.8 and 0.40 ± 0.09 mg protein/g liver), recoveries were calculated from the EGFR content of the total particulate fraction (*vide supra*). The recovery of the plasma membrane fraction was thus calculated as 30.5%, and the GE fraction as 16%.

Electron microscopy of plasma membrane and GE fractions

For electron microscopy, subcellular fractions (50 μg cell fraction protein) were harvested and fixed immediately (*vide infra*). Fractions were fixed in 2.5% glutaraldehyde, 100 mM sodium cacodylate (pH 7.4) at 4°C. Samples were filtered under N_2 onto Millipore nitrocellulose filters (0.45 μm) (Millipore–Waters, Mississauga, Ontario, Canada) utilizing the filtration apparatus described by Baudhuin *et al.* (1967). Filters were post-fixed in 2% OsO_4, 100 mM cacodylate buffer (pH 7.4), and stained *en bloc* with 1% tannic acid (Simionescu and Simionescu, 1976), 8% uranyl acetate, 100 mM maleic buffer, pH 5 (Karnovsky, 1967), and processed for routine electron microscopy.

Immunoprecipitation

To immunoprecipitate the EGFR and SHC, subcellular fractions were solubilized with 1% TX-100, 0.5% deoxycholate, 10% glycerol in HBS (50 mM HEPES, pH 7.5, 150 mM NaCl) for 30 min at 4°C. The fractions were centrifuged at top speed for 5 min in a Brinkmann microfuge. 10 μg of monoclonal EGFR antibody (IgG 151 BH-6) or anti-SHC antibodies were added to the supernatants and incubated for 2 h at 4°C. The immune complex was precipitated using protein A–Sepharose for 60 min at 4°C. The beads were then washed three times with solubilizing buffer and once with HBS.

Immunoblotting

Samples were boiled in Laemmli sample preparation buffer (Laemmli, 1970) for 5 min, electrophoresed on 8 or 10% (for GRB2 immunoblots) polyacrylamide gels and transferred onto nitrocellulose (Xymotech, Mt Royal, Quebec, Canada). The blots were incubated in 5% skimmed milk in TNT buffer (0.15 M NaCl, 0.05% Tween-20, 10 mM Tris, pH 7.5) or 2% BSA/TNT (for phosphotyrosine immunoblots). Antibodies to GRB2, phosphotyrosine, mSOS and Raf-1 were used at the dilutions suggested by the manufacturers. Bands were visualized with [^{125}I]goat anti-mouse or [^{125}I]goat anti-rabbit secondary antibodies (300 000 c.p.m./ml) and exposed to Kodak X-OMAT X-ray film. Polyclonal antibodies raised to SHC, EGFR and Pep(P) were used at dilutions of 1:1000, 1:1000 and 1:750, respectively. Visualization was carried out with [^{125}I]goat anti-rabbit secondary antibody (300 000 c.p.m./ml) and exposed to Kodak X-OMAT X-ray film. Quantitation was carried out using a BAS 2000 Fuji Bio-Imaging Analyzer (Fuji BioMedical Systems, Inc., Bethseda, MD), with the gradation, resolution and sensitivity settings as described by the manufacturer for immunoblots. Immunoblots containing radiolabeled secondary antibody were exposed to the phosphoimaging plate for 15 (SHC), 60 (EGFR), 80 (phosphotyrosine) and 120 min (GRB2), and radioactivity was quantified as arbitrary units. Alkaline phosphatase-conjugated secondary antibodies, either to the whole molecule or to heavy chain-specific (for GRB2 and mSOS immunoblots), were used to visualize immunoblots of immunoprecipitations as described for immunostaining by Smith and Fisher (1984).

Acknowledgements

The first two authors contributed equally to this work. We would like to thank Dr W.H.Lai (McGill University) for the electron microscopy work and Drs J.McGlade, T.Pawson (Mount Sinai Hospital, University of Toronto) and G.Pelicci (University of Perugia, Italy) for their generous gift of the anti-SHC antibody and the pGEX–SHC SH2 construct. We would also like to thank Dr D.Stern (Yale University) for the Pep(P) antibody, Dr J.Schlessinger (New York University College of Medicine) for communicating to us his results prior to publication, and Mrs S.Benchimol and Dr C.P.Stanners (McGill Cancer Center, McGill University) for the use of the BAS2000 phosphoimager. We also acknowledge Dr P.A.Walton (McGill University) who kindly reviewed this manuscript prior to submission. This work was supported by the NCI of Canada. This paper is dedicated to the memory of Dr W.H.Lai.

References

Authier,F., Rachubinski,R.A., Posner,B.I. and Bergeron,J.J.M. (1994) *J. Biol. Chem.*, **269**, 3010–3016.

Backer,J.M., Kahn,C.R. and White,M.F. (1990) *J. Biol. Chem.*, **265**, 14828–14835.

Baltensperger,K., Kozma,L.M., Cherniack,A.D., Klarlund,J.K., Chawla,A., Banerjee,U. and Czech,M.P. (1993) *Science*, **260**, 1950–1952.

Bangalore,L., Tanner,A.J., Laudano,A.P. and Stern,D.F. (1992) *Proc. Natl Acad. Sci. USA*, **89**, 11637–11641.

Batzer,A.G., Rotin,D., Ureña,J.M., Skolnik,E.Y. and Schlessinger,J. (1994) *Mol. Cell. Biol.*, **14**, 5192–5201.

Baudhuin,P., Evrard,P. and Berthet,J. (1967) *J. Cell Biol.*, **32**, 181–191.

Bergeron,J.J.M., Rachubinski,R., Searle,N., Borts,D., Sikstrom,R. and Posner,B.I. (1980) *J. Histochem. Cytochem.*, **28**, 824–835.

Bergeron,J.J.M., Searle,N., Khan,M.N. and Posner,B.I. (1986) *Biochemistry*, **25**, 1756–1764.

Buday,L. and Downward,J. (1993) *Cell*, **73**, 611–620.

Burgess,J.W., Wada,I., Ling,N., Khan,M.N., Bergeron,J.J.M. and Posner,B.I. (1992) *J. Biol. Chem.*, **267**, 10077–10086.
Chang,C.-P. *et al.* (1993) *J. Biol. Chem.*, **268**, 19312–19320.
Chardin,P., Camonis,J.H., Gale,N.W., Aelst,L.V., Schlessinger,J., Wigler,M.H. and Bar-Sagi,D. (1993) *Science*, **260**, 1338–1343.
Cohen,S., Fava,R. and Sawyer,S.T. (1982) *Proc. Natl Acad. Sci. USA*, **79**, 6237–6241.
Doherty,J.-J.,II, Kay,D.G., Lai,W.H., Posner,B.I. and Bergeron,J.J.M. (1990) *J. Cell Biol.*, **110**, 35–42.
Donaldson,R.W. and Cohen,S. (1992) *Proc. Natl Acad. Sci. USA*, **89**, 8477–8481.
Downward,J., Parker,P. and Waterfield,M.D. (1984) *Nature*, **311**, 483–495.
Egan,S.E., Giddings,B.W., Brooks,M.W., Buday,L., Sizeland,A.M. and Weinberg,R.A. (1993) *Nature*, **363**, 45–51.
Faure,R., Baquiran,G., Bergeron,J.J.M. and Posner,B.I. (1992) *J. Biol. Chem.*, **267**, 11215–11221.
Felder,S., Miller,K., Moehren,G., Ullrich,A., Schlessinger,J. and Hopkins,C.R. (1990) *Cell*, **61**, 623–634.
Gale,N.W., Kaplan,S., Lowenstein,E.J., Schlessinger,J. and Bar-Sagi,D. (1993) *Nature*, **363**, 88–92.
Geuze,H.J., Slot,J.W., Strous,G.J.A.M., Peppard,J., von Figura,K., Hasilik,A. and Schwartz,A.L. (1984) *Cell*, **37**, 195–204.
Hsuan,J.J., Totty,N. and Waterfield,M.D. (1989) *Biochem. J.*, **262**, 659–663.
Jhappan,C., Stahle,C., Harkins,R.N., Fausto,N., Smith,G.H. and Merlino,G.T. (1990) *Cell*, **61**, 1137–1146.
Kahn,C.R., Freychet,P., Roth,J. and Neville,D.M.,Jr (1974) *J. Biol. Chem.*, **249**, 2249–2257.
Karnovsky,M.J. (1967) *J. Cell Biol.*, **35**, 213–236.
Kay,D.G., Lai,W.H., Uchihashi,M., Khan,M.N., Posner,B.I. and Bergeron,J.J.M. (1986) *J. Biol. Chem.*, **261**, 8473–8480.
Kelly,K.L. and Ruderman,N.B. (1993) *J. Biol. Chem.*, **268**, 4391–4398.
Khan,M.N., Savoie,S., Bergeron,J.J.M. and Posner,B.I. (1986) *J. Biol. Chem.*, **261**, 8462–8472.
Khan,M.N., Baquiran,G., Brule,C., Burgess,J., Foster,B., Bergeron,J.J.M. and Posner,B.I. (1989) *J. Biol. Chem.*, **264**, 12931–12940.
Laemmli,U.K. (1970) *Nature*, **227**, 680–685.
Lai,W.H., Cameron,P.H., Wada,I., Doherty,J.-J.,II, Kay,D.G., Posner,B.I. and Bergeron,J.J.M. (1989a) *J. Cell Biol.*, **109**, 2741–2749.
Lai,W.H., Cameron,P.H., Doherty,J.-J.,II, Posner,B.I. and Bergeron,J.J.M. (1989b) *J. Cell Biol.*, **109**, 2751–2760.
Li,N., Batzer,A., Daly,R., Yajnik,V., Skolnik,E., Chardin,P., Bar-Sagi,D., Margolis,B. and Schlessinger,J. (1993) *Nature*, **363**, 85–88.
Lowenstein,E.J. *et al.* (1992) *Cell*, **70**, 431–442.
Margolis,B.L., Lax,I., Kris,R., Dombalagian,M., Honegger,A.M., Howk,R., Givol,D., Ullrich,A. and Schlessinger,J. (1989) *J. Biol. Chem.*, **264**, 10667–10671.
Marti,U., Burwen,S.J. and Jones,A.L. (1989) *Hepatology*, **9**, 126–138.
McCormick,F. (1993) *Nature*, **363**, 15–16.
Mead,J.E. and Fausto,N. (1989) *Proc. Natl Acad. Sci. USA*, **86**, 1558–1562.
Morrison,D.K., Kaplan,D.R., Escobedo,J.A., Rapp,U.R., Roberts,T.M. and Williams,L.T. (1989) *Cell*, **58**, 649–657.
Mortimore,G.E., King,E.,Jr, Mondon,C.E. and Glinsmann,W.H. (1967) *Am. J. Physiol.*, **212**, 179–183.
O'Keefe,E., Hollenberg,M.D. and Cuatrecasas,P. (1974) *Arch. Biochem. Biophys.*, **164**, 518–526.
Olivier,J.P., Raabe,T., Henkemeyer,M., Dickson,B., Mbamalu,G., Margolis,B., Schlessinger,J., Hafen,E. and Pawson,T. (1993) *Cell*, **73**, 179–191.
Pelicci,G. *et al.* (1992) *Cell*, **70**, 93–104.
Pronk,G.J., McGlade,J., Pelicci,G., Pawson,T. and Bos,J.L. (1993) *J. Biol. Chem.*, **268**, 5748–5753.
Rothenberg,P.L., Lane,W.S., Karasik,A., Backer,J., White,M. and Kahn,C.R. (1991) *J. Biol. Chem.*, **266**, 8302–8311.
Rozakis-Adcock,M. *et al.* (1992) *Nature*, **360**, 689–692.
Rozakis-Adcock,M., Fernley,R., Wade,J., Pawson,T. and Bowtell,D. (1993) *Nature*, **363**, 83–92.
Ruff-Jamison,S., McGlade,J., Pawson,T., Chen,K. and Cohen,S. (1993) *J. Biol. Chem.*, **268**, 7610–7612.
Simionescu,N. and Simionescu,M. (1976) *J. Cell Biol.*, **70**, 608–621.
Simon,M.A., Dodson,G.S. and Rubin,G.M. (1993) *Cell*, **73**, 169–177.
Skolnik,E.Y., Batzer,A., Li,N., Lee,C.H., Lowenstein,E., Mohammadi,M., Margolis,B. and Schlessinger,J. (1993a) *Science*, **260**, 1953–1955.
Skolnik,E.Y. *et al.* (1993b) *EMBO J.*, **12**, 1929–1936.
Smith,D.E. and Fisher,P.A. (1984) *J. Cell Biol.*, **99**, 20–28.
Sorkin,A. and Carpenter,G. (1993) *Science*, **261**, 612–615.
Ueki,K. *et al.* (1994) *J. Biol. Chem.*, **269**, 15756–15761.
Wada,I., Lai,W.H., Posner,B.I. and Bergeron,J.J.M. (1992) *J. Cell Biol.*, **116**, 321–330.
Walton,G.M., Chen,W.S., Rosenfeld,M.G. and Gill,G.N. (1990) *J. Biol. Chem.*, **265**, 1750–1754.
Wood,K., Sarnecki,C., Roberts,T.M. and Blenis,J. (1992) *Cell*, **68**, 1041–1050.

Received on March 22, 1994; revised on July 4, 1994